JPET Fast Forward. Published on September 27, 2010 as DOI: 10.1124/jpet.110.171983

JPET # 171983

Intracellular GSH Depletion Triggered Mitochondrial Bax Translocation to Accomplish Resveratrol Induced apoptosis in U937 cell Line

Prasun Guha, Anindya Dey, Rupashree Sen, Mitali Chatterjee, Subrata Chattopadhyay and Sandip. K. Bandyopadhyay

Affiliations:

Department of Biochemistry, Dr. B.C. Roy Post Graduate Institute of Basic medical Sciences & I.P.G.M.E.&R, 244B, Acharya Jagadish Chandra Bose Road, Kolkata-700020, India (**P. G., A. D. and S. K. B.**), Department of Pharmacology, Dr. B.C. Roy Post Graduate Institute of Basic medical Sciences & I.P.G.M.E.&R, Kolkata-700 020 (**R. S. and M. C.**), Bio-Organic Division, Bhabha Atomic Research Centre, Mumbai - 400 085, India **(S. C.)**

Running Title Page

Running title: Resveratrol triggered GSH depletion and Bax translocation

Address correspondence to: Dr. Sandip K. Bandyopadhyay, Department of Biochemistry, Dr. B.C. Roy Post Graduate Institute of Basic medical Sciences & I.P.G.M.E.&R, 244B, Acharya Jagadish Chandra Bose Road, Kolkata-700 020, India. Phone: 91-033-22234838; Fax: 91-033-22234844; E-Mail: sandipkpc@gmail.com.

Number of Text Pages: 28

Number of Tables: 0

Number of figures: 6

Number of references: 18

Number of words in abstract: 198

Number of words in introduction: 396

Number of words in Discussion: 1058

Non-standard Abbreviations: Resv, resveratrol; HST-1, hydroxstilbene-1; GSH, glutathione, GSSG; oxidized glutathione; ROS; reactive oxygen species,PEG, ploye thyl glycol;

Section selected: CELLULAR AND MOLECULAR

Abstract

We have previously demonstrated that Resveratrol (Resv) induced cellular apoptosis occurs following formation of ROS, but the role of GSH has not been well defined. Our experimental data enumerated that Resv treatment (50μm) induced apoptosis in U937 cell which was preceded by cellular GSH efflux. High concentration of extra cellular thiol (GSH, NAC) and two specific inhibitors of carrier mediated GSH extrusion; methionine or cystathionine prevented the process of oxidative burst and cell death. Thus proved that GSH efflux could be a major molecular switch to modulate Resv induced ROS generation. Spectrofluorimetric data depicted that after 6 h of Resv treatment ROS generation was evident. Pre-treatment of cells with intracellular ROS scavenger (PEG-SOD and PEG-Catalase) efficiently reduced ROS generation but failed to prevent intracellular GSH depletion. Thus, it suggested that intracellular GSH depletion was independent of ROS production but dependent on GSH extrusion. Furthermore, to bridge the link between GSH efflux and ROS generation we carried out confocal microscopy of the localization of Bax protein. Microscopic analysis and siRNA treatment emphasized that cellular GSH efflux triggered Bax translocation to mitochondria which resulted in the loss of mitochondrial membrane potential, ROS generation and caspase 3 activation thus triggered apoptosis.

Introduction

Oxidants have been widely shown to initiate the cellular apoptotic cascade by perturbing the balance between cellular signals for survival and suicide. Glutathione (GSH) is the most abundant intracellular low molecular weight thiol, and is among the many detoxification processes that maintains cellular redox homeostasis. Its protective action is based on oxidation of the thiol group of its cysteine residue, resulting in the formation of GSSG; this in turn is catalytically reversed to GSH by glutathione reductase (Meister *et al*., 1983). Under conditions of oxidative stress, GSSG may either recycle to GSH or exit from the cells, leading to an overall depletion of glutathione (Reed *et al*., 1990). Glutathione can also be extruded in the reduced form, through specific carriers, by many cell types under physiological conditions.

Intracellular loss of GSH is an early hallmark in the progression of cell death in response to different apoptotic stimuli (Hammond *et al*., 2004; Franco *et al*., 2006) and has been associated with activation of a plasma membrane transport mechanism rather than to its oxidation (van den Dobbelsteen *et al*., 1996; He *et al*., 2003). Several studies have also shown a correlation between cellular depletion of GSH and progression of apoptosis (Ghibelli *et al*., 1998; Franco *et al*., 2006). We have already reported that treatment with Resv stimulates production of reactive oxygen species (ROS) leading to a caspase dependent apoptosis in U937 cell line (Guha *et al*., 2010). However, the characterization of the nature of ROS generated (hydrogen peroxide or peroxynitrite or singlet oxygen or hydroxyl radical) and the effect of Resv on intracellular level of GSH was not explored. At the same time it has already been reported that generation of ROS is

modulated by translocation of mitochondrial Bax (Kirkland *et al*., 2007). Bax is a proapoptotic Bcl_2 family of protein wherein apoptotic stimuli stimulates mitochondrial Bax translocation leading to dissipation of the mitochondrial membrane potential and generation of ROS. Recently, (Honda *et al*., 2004) emphasized that intracellular GSH depletion enhanced mitochondrial Bax translocation resulting in apoptosis. As stated by. (Mohan *et al.* 2006), Resv induced Bax activation is an upstream event in apoptosis but the exact link between GSH depletion, ROS generation, and mitochondrial Bax translocation has not been specified. Hence, here we tried to draw a correlation between depletion of intracellular GSH, production of ROS and translocation of mitochondrial Bax in Resv induced apoptotic cell death.

Materials and Methods

Reagents and kits - All chemicals were obtained from Sigma-Aldrich (St. Louis, MO) except primary antibodies (Bax, β-actin, COX IV) and polyclonal secondary antibody were obtained from Cell Signaling Technology (USA), Apo-direct TUNEL ASSAY KIT, and caspase protease assay kit, were purchased from Millipore (Temecula, CA, USA), Alexa fluor 488-AnnexinV/PI kit, CM-H_2DCFDA, Singlet Oxygen Sensor Green dye, RPMI 1640, Fetal Bovine Serum (FBS), penicillin-streptomycin, trypsin-EDTA, from Invitrogen, USA, Mitochondria/Cytosol fractionation kit, GSH assay kit from BioVision (Mountain View, USA). . Revert Aid H minus first strand cDNA synthesis kit and Dynamo SYBR Green quantitative PCR kit (MBI Fermentas, Hanover, MD).

Cell culture - U937 (human leukemic monocyte lymphoma), cell line was obtained from National Centre for Cell Science (NCCS), Pune, India. U937 was cultured in RPMI 1640, at pH 7.4. Media was supplemented with 10% fetal bovine serum and antibiotics (100 U/ml penicillin-G, 100µg/ml streptomycin, and 6 µg/ml Gentamycin). The cells were incubated at 37^{o}C in a humidified atmosphere containing 5% $CO_{2;}$. Cells were subcultured weekly and cells from passages 6 to 8 were used for experiments.

CellTiter-Glo® Luminescent Cell Viability Assay - The CellTiter-Glo® Luminescent Cell Viability Assay was used to determine cell viability based on quantitation of the ATP present, which signals the presence of metabolically active cells. Briefly, cells (5 X10^{4} cells/100 µl medium/well) were seeded in 96-well plates and incubated for12, 24, 48 and 72 h.in the presence of Resv (dissolved in 0.02-0.07% DMSO); each well was then treated with a volume of CellTiter-Glo® Reagent equal to the volume of cell culture medium present, mixed for 2 minutes on an orbital shaker to induce cell lysis and incubated at room temparature for 10 min. after which the stabile luminescent signal was reordered in a luminometer (BioTek, FLX800, USA).

Detection of apoptosis by AnnexinV/PI double staining method - Perturbations in the cellular membrane occur during the early stage of apoptosis and lead to a flippage of phophotidyl serine to the external aspect of the cell membrane. Annexin V selectively binds to phosphatidyl serine and helps identify cells undergoing apoptosis. Cells were treated with different concentration of Resv for 24 h and apoptosis was measured using AnnexinV Alexa fluor 488 and-PI Apoptosis Detection Kit. Briefly, U937 cells were harvested and PI (5 µl) and Annexin V Alexa fluor 488 (5 µl) was added, incubated for 15 min. at room temparature in the dark, and then analyzed on a flowcytometer (equipped

with 488 nm argon laser light source, 515 nm band pass filter for Alexa fluor 488 and 623 nm band pass filter for PI fluorescence) using CellQuest software; a total of 10,000 events were acquired

TUNEL assay - To confirm the nature of tumor killing by Resv on U937 cells were fixed, permeabilized and incubated with TdT (terminal deoxynucleotidyl transferase) enzyme and FITC- dUTP as per the manufacturer's instructions. Cells were then washed, incubated with RNAase solution and acquired on a flow cytometer (Becton Dickinson, San Diego CA, USA) which was equipped with 488 nm Argon laser light source; 515 nm band pass filter, FL1-H) and analyzed using CellQuest software.

Measurement of mitochondrial membrane potential - The loss of mitochondrial membrane potential (MMP) is a hallmark for apoptosis. It is an early event preceding phosphatidylserine externalization and coinciding with activation of caspases. MMP was measured using a JC-1 kit following the manufacturer's protocol. The mitochondrial membrane potential detection kit uses a unique fluorescent cationic dye, JC-1 (5,5'6,6'-tetracholoro-1,1',3,3'-tetraethyl- benzimidazolylcarbo cyanine iodide) (excitation 488 nm and emission 525 nm), to signal the loss of MMP. Cells were harvested at different time points (0.5, 1, 3, 6, 12, 24, 48 h) of Resv treatment. Then mitochondrial permeability transition was determined by staining of the cells with JC-1. Briefly, cells (1x106) were incubated with JC-1 (2.5µg/ml in 1 ml PBS) for 30 min at 37ºC with moderate shaking. Cells were then centrifuged (1000x g, 4ºC for 5 min), washed twice with ice-cold PBS and finally resuspended in 200 µl PBS. Mitochondrial permeability transition was subsequently quantified on a spectrofluorimeter (JASCO, Japan FP6300) and data are given in the ratio of (590/530).

Preparation of cytosolic and mitochondrial fractions - U937 cells were harvested after treatment with Resv. Isolation of a highly enriched mitochondrial and cytosolic fraction of cells was performed using a mitochondria/cytosol fractionation kit. Briefly, cells (5 x 10^7) were washed twice in ice-cold PBS, resuspended in 1.0 ml of cytosol extraction buffer mix containing DTT and protease inhibitors and incubated on ice for 10 min. The cells were homogenized on ice, centrifuged (700 x g for 10 min at 4°C) and the resultant supernatant was then centrifuged at 10,000 x g for 30 min at 4°C. The supernatant along with the pellet that was resuspended in 0.1 ml mitochondrial extraction buffer mix containing DTT and protease inhibitors, vortexed for 10 sec were and stored as the cytosolic and mitochondrial fraction respectively and subjected to western blot analysis.

Caspase activation assay - Caspase-3 was assayed by flow cytometry using CaspaTag™ Caspase-3 in Situ Assay Kit, Fluorescein (Millipore, USA) as per the manufacturer's instructions.

Western blot analysis - Cell lysates were prepared using a mammalian cell lysis kit MCL1 (Sigma, USA) containing 5X Tris-EDTA buffer, 5X NaCl buffer, 5X SDS (lauryl sulfate) buffer, 5X DOC (deoxycholic acid) buffer, 5X Igepal CA 630 buffer and Protease inhibitor cocktail. To prepare 1 ml cell lysis buffer for the extraction of 10^6-10^7 cells each of the buffer was taken in 200 µl volume and protease inhibitor cocktail was used at a 1:100 dilution in the cell lysis buffer. Briefly, cells were immersed in freshly prepared lysis buffer with protease inhibitor cocktail, sonicated and centrifuged (12,000 X g for 10 min) and the protein concentration of the supernatant was measured (Bradford *et al*., 1976). Cellular proteins (50 µg) were resolved by 10% non-reducing SDS-polyacrylamide gel electrophoresis, and transferred to nitrocellulose membranes. The

membranes were blocked for 2 h at room temperature in 20 mM Tris-HCl, pH 7.4, 150 mM NaCl, 0.02% Tween 20 (TBST) containing 3% BSA followed by overnight incubation at 4°C in 1:500 dilution of the respective antibodies for Bax, β-actin and COX IV. The membranes were washed thrice with TBST, incubated with alkaline phosphatase-conjugated secondary antibody, and the bands visualized using a 5-bromo-4-chloro-3-indolyl phosphate/nitro blue tetrazolium substrate.

Confocal imaging of localization of Bax on mitochondria - U937 cells were fixed with 4% paraformaldehyde for 15 min. followed by two steps of washing with PBS. Cells were then permeablized with 0.1% triton X 100 for 4 min. followed by two washings with PBS. Mitochondria were stained using COX IV alexa fluor 488 monoclonal antibody (diluted 1: 100) along with Bax primary antibody (1: 100) followed by Alexa fluor 594 anti mouse secondary antibody (1: 300). After washing, the cells were mounted by gold antifade mounting medium and examined under a confocal microscope (Nikon). The bar depicted the magnificantion 10μm.

Transfection of siRNA of Bax - siRNA for Bax and negative control siRNA were purchased from AMBION and transfection of 5nM siRNA were carried out using amine transfection assay kit from ambion. All Bax depletions were carried out using Silencer® Select Validated siRNA for Bax ID s1889 (AppliedBiosystem., Foster city ,CA, USA) 16 h after transfection. Silencer® Select Negative Control #2 siRNA (AppliedBiosystem., Foster city ,CA, USA) was included in each experiment. Cells were washed in medium containing serum, adjusted to 5×10^4 cells/ml in RPMI 1640 supplemented with 10% fetal bovine serum. 5×10^4 cells in a 400 μl volume were transfected with siRNA by amine transfection method.

RNA isolation and TaqMan Real time-PCR to validate the transfection of Bax siRNA - After extracting the total RNA using Gen Elute Mammalian Total RNA miniprep kits (Sigma), and checking its integrity by electrophoresis, the cDNA was synthesized from 5 mg of purified total RNA using Revert Aid H minus firststrand cDNA synthesis kit (Fermentas Life Sciences, Ontario, Canada). quantitative real-time PCR was performe on ABI prism 7900HT sequence detection system (AppliedBiosystem., Foster city, CA, USA) using Taqman gene master mix(Part number 4304437) and pre-developed TaqMan assay specific to human Bax (Hs00751844_s1, FAM/MGB primer Ltd) and for the house keeping gene 18s (4319413E, VIC/MGB, primer Ltd) in a duplex reaction of final volume 10 µl. amplification condition const of UNG activation (uracyl-N-glycosidase) at 50 oc for 2 mins and initial DNA Polymerase activation at 95 oc FOR 10 mins followed by 40 cycles of denaturation at 95oc for 15 sec and annealing/ extension at 60oc for 1 min. Total time required (1h 48 mins). The samples were quantified for all the above genes using the comparative Ct ($^{\Delta\Delta}$Ct) method, as described in the Assays-on-Demand Users Manual (Applied Biosystem, Foster city, CA, USA).

Measurement of intracellular GSH - Intracellular GSH was measured spectrofluorimetrically using ApoGSH^{TM} Glutathione Detection Kit (BioVision, USA). In brief, the treated and control cells (1 X 10^6) were collected into 1.5 ml microcentrifuge tubes and centrifuged at 700 x g for 5 minutes to remove the supernatant. Then the cell pellets was lysed in 100 µl ice-cold Cell Lysis Buffer. After this it was incubated on ice for 10 minutes, then centrifuged at top speed in an eppendorf centrifuge for 10 minutes and the cell lysate was transferred into new tubes for glutathione assay. Assay samples were diluted with Cell Lysis Buffer to total volume of 100 µl. 2 µl of the 50 U/ml GST

Reagent and 2 µl of MCB (monochloribimane) dye was added into each samples and incubated the reaction at 37 ^{o}C for 30 min.Then the fluorescence value was measured in a fluorescence plate reader at Ex./Em. = 380/460 nm. The result was expressed in ng/ml of sample.

Detection of reactive oxygen species (ROS) - ROS was measured by CM H_2DCFDA (Invitrogen, USA) (Ex 490 nm, Em 527 nm) (Guha *et al*., 2010) and singlet oxygen was measured by Singlet Oxygen Sensor Green dye (Ex 488, Em 525). The cells were preloaded with these dyes respectively and their reactivity with ROS analyzed spectrofluorimeterically.

Statistical analysis - Data were expressed as mean ± S.D. otherwise before mentioned. Comparisons were made between different treatments (analysis of variance) using the software GraphPad InStat (GraphPad Software Inc., San Diego, CA), where an error protecting the multiple comparison procedure, namely Tukey-Kramer multiple comparison tests, was applied for the analysis of significance of all the data.

Results

Resv treatment induced apoptosis in U937 cell line - The antiproliferative effect of Resv was examined and evaluated on U937 cell lines using the CellTiter-Glo® Luminescent Cell Viability Assay kit. Our study revealed that a significant ($p < 0.001$) reduction in cell viability was evident at 48 h of Resv treatment (Figure 1A). The IC_{50} values of Resv at the dose of 50 µM exerted profound cytotoxic effect after 48h of treatment on U937 cell line. Therefore, further experiments were performed at the IC_{50} dose of Resv.

To study the nature of cell death, cells were treated for 24 h, stained with Anexin V Alexa fluor 488/PI, and analyzed by FACS. In the early stages of apoptosis, while the cell membrane remains almost intact, PI (propidium iodide) cannot permeate inside the cells and remains unable to stain the DNA. However, at the early phase of apoptosis, phosphatidylserine, to which Annexin V binds specifically, is translocated to the extra-cellular leaflet of the membrane. In contrast, during necrosis, because the cell membrane is ruptured, these cells take up only PI. Our flowcytometric data revealed that, in comparison with vehicle treated control (0.02% DMSO), Resv treated unfixed U937 cells showed Annexin V- Alexa fluor 488-binding but PI staining was insignificant (Figure 1B) indicating that the mode of cell death was apoptosis, not necrosis. Further, DNA fragmentation by means of TUNEL assay and caspase 3 activation after 48h of Resv treatment proved that the mode of cell death was majorly apoptosis (Figure 1C, D).

Resv treatment modulated dissipation of mitochondrial membrane potential and induced ROS generation - Caspase 3 activation indicated the involvement of mitochondrial death cascade in apoptosis. We therefore investigated the dissipation of mitochondrial membrane potential ($\Delta\Psi m$) in Resv treated U937 cells. Spectrofluorimetric data indicated that ($\Delta\Psi m$) dissipation was evident from 1h of treatment and increased in a time dependent manner (Figure 2A). Change in ($\Delta\Psi m$) is concomitantly related with the intracellular ROS production (Macho *et al*., 1997). Our spectrofluorimetric study elucidated that ROS generation was significantly evident after 6 h of Resv treatment and maintained up to 12 h (Figure 2B).

Resv treatment triggered oxidative burst in mitochondria and production of H_2O_2 resulted in the deleterious effects - According to Schimmel *et al*, extracellular ROS

exhibits a strong apoptosis-inducing potential in different cancer cells. Membrane associated NADPH oxidase seems to be the key enzynme responsible for generation of ROS (Schimmel *et al*., 2002). Here, we tried to delineate whether extracellular ROS would exhibit pro-apopotic functions in Resv induced cell death. The pretreatment of cells with a specific NADPH oxidase inhibitor apocyanin (200 μM) failed to impart any significant effects on Resv induced ROS generation and cell death (Figure 3A) thus confirming that the extracellular ROS generating system did not contribute towards Resv induced ROS production. The effect of apocyanin was also evaluated in a dose dependent manner but no significant change was noticed (data not shown). The characterization of the type of ROS was also evaluated consequently. The increased fluorescence intensity of CM-H_2DCFDA proved that significant production of H_2O_2 occurred in Resv treated U937 cells which was efficiently scavenged by cell permeable PEG-SOD, PEG-catalase, and NAC as shown in Figure 3B. In unison treatment with PEG-SOD reduced CM-H_2DCFDA fluorescence level in a dose dependent fashion (supplementary Figure 2) thus proved the role of superoxide. Superoxide can produce H_2O_2 and hydroxyl radicals (.OH). Dose dependent study (supplementary Figure 3)DMTU (.OH scavenger) at the dose of 6 mM efficiently prevented cell death after Resv treatment (Figure 3C) thus proved that Resv treatment instigated mitochondrial superoxide production which consequently through downstream reactions produced H_2O_2 and .OH. However, we failed to detect singlet oxygen ($^1O_2$) (assessed with the Singlet Oxygen Sensor Green dye) (Figure 3D) and the pretreatment of NOS inhibitor L-NAME (1 mM) also signified no role of peroxynitrate after Resv treatment (Figure 3E). The effect of L-NAME was also evaluated in a dose dependent manner but no significant change was noticed (data not

shown). Thus, the data characterized that mitochondria was the important ROS producing machinery and the type ROS was majorly superoxide which intern produced reactive (.OH) and H_2O_2.

Generation of ROS was modulated by efflux of GSH - Glutathione (GSH) depletion is an early hallmark observed in H_2O_2 dependent apoptosis. We therefore investigated the GSH status after the treatment of Resv. Time dependent study elucidated that GSH depletion was significant from almost initial hours of treatment and increased with the time (Figure. 4A).

Most studies suggest that GSH depletion during apoptosis is an indicator for ROS formation and oxidative stress. Such findings have led to the widespread assumption that GSH depletion is a byproduct of the apoptotic process; and that ROS formation and GSH depletion in apoptosis are coupled together as cause and consequence phenomena. We next analyzed the role of ROS on the modulation of GSH depletion by the use of a variety of antioxidants. Hydrogen peroxide (H_2O_2) formation induced by Resv was prevented in the presence of PEG-SOD and PEG-Cat (Figure 3B upper panel), which acts as a potent intracellular scavenger for H_2O_2. However, scavenging of the ROS generated upon Resv treatment by these antioxidants, did not significantly affect GSH depletion. Where as, pretreatment of cells with NAC (8mM) or supplementation of the media with GSH (5 mM) prevented the intracellular GSH depletion (Figure 4B). To gain a better insight into the control of GSH depletion we pretreated the cells with two specific inhibitors of carrier mediated GSH extrusion; cystathionine (1mM) and methionine (1mM), which significantly prevented the intracellular GSH depletion (Figure 4C). As indicated in Figure 4D-F, pretreatment of cells with extracellular thiol (NAC 8mM and

GSH 5 mM) or cystathionine (1 mM) not only inhibited GSH efflux, but also prevented the loss of ($\Delta\Psi m$), and decreased cell death number. These results suggested a causative role for GSH efflux in Resv induced apoptosis.

Resv induced Bax translocation to mitochondria was modulated by GSH depletion - Although, GSH efflux was independent of ROS production but intracellular ROS formation could be a sequential effect after GSH extrusion. After Resv treatment total Bax expression remained unchanged compared to control however western blot data of cytosolic and mitochondrial lysate clearly emphasized the phenomenon of mitochondrial Bax translocation (Figure 5A). This was further validated by confocal microscopy (color picture of Bax translocation has been given in supplementary Figure 4). Our confocal imaging study enumerated significant amount of Bax translocation in mitochondria within 6 h of Resv treatment (Figure 5B). To get a link between GSH efflux and mitochondrial Bax translocation we initially treated the cells with BSO (1 mM) an irreversible inhibitor of gamma-glutamylcysteine synthetase. BSO and Resv treatment stimulated the mitochondrial Bax translocation after 6 h but treatment of NAC and cystathionine significantly prevented translocation of Bax to mitochondria in Resv treated cell (Figure 5), however further addition of BSO reversed this protective effect , thus suggested, GSH depletion stimulated mitochondrial Bax translocation in Resv treated U937 cell line.

Bax translocation triggered mitochondrial death signal - To bridge the link between GSH extrusion, Bax translocation and mitochondrial apoptotic signal the cells were treated with siRNA of Bax protein. The activity of siRNA was validated by real time-PCR data (Figure 6A). From (Figure 6B) it was evident that Bax siRNA treatment

minimized the amount of cell death by 47 %, which was well evident with the inhibition of caspase 3 activation (Figure 6C). To gain a better insight into the contribution of Bax in the oxidative burst and depletion of ($\Delta\Psi$m) we analyzed the amount of ROS generation and loss of ($\Delta\Psi$m) in the Bax siRNA treated cells. Experimental data enumerated that in Resv treated cell Bax siRNA significantly reduced ROS production (Figure 6D) and prevented the dissipation of ($\Delta\Psi$m) (Figure 6E).

Discussion

Changes in the intracellular redox environment of cells have been reported to be critical for the activation of apoptotic enzymes and the progression of programmed cell death. Small thiols, including glutathione are viewed as protective antioxidants acting as free radical scavengers in response to oxidative damage; thus, being important players in the redox balance of the cell. Glutathione depletion has been shown to occur in apoptosis induced by a wide variety of stimuli, and has been shown mediated by its extrusion and its oxidation. However, Franco *et al* and Ghibelli *et al* (Ghibelli *et al*., 1998; Franco *et al*., 2007) have emphasized that GSH efflux but not the GSH oxidation was one of the important events in apoptosis.

It had already been proved that Resv induced apoptosis were mostly ROS driven (Guha *et al*., 2010); however, the exact role of GSH in ROS generation and cell death had not yet been explored. Therefore, here we tried to investigate the effect of Resv on modulation of GSH level and its probable role in Resv induced apoptosis in U937 cells.

Luminometric cell viability study depicted that Resv showed its antiproliferative effects in a time dependent manner and IC_{50} value came around 48 h of treatment at the dose of 50 μM (Figure 1A). Further, flowcytometric analysis for Anexin V and TUNEL assay proved apoptotic mode of cell death which was supported by activation of caspase 3 also (Figure 1B, C, D). Aactivation of caspase 3 helped to presume the role of mitochondria in Resv treated apoptosis.

Fluorimetric investigations suggested that Resv treatment started to dissipate mitochondrial membrane potential ($\Delta\Psi m$) rapidly within 1 h of treatment and continued in a time dependent manner (Figure 2A). However, time dependent study illustrated that ROS generation was significant after 6 h of Resv treatment and maintained up to 12 h (Figure 2B). Although within 3 h of Resv treatment a trend of oxidative burst was evident but pretreatment of cells with PEG-SOD or PEG-Cat failed to prevent the dissipation of ($\Delta\Psi m$) (Supplementary data 1). So from these data it was clear that loss of ($\Delta\Psi m$) was independent of ROS generation.

Although, mitochondria are considered to be the major source of ROS still extracellular superoxide anion generation through membrane associated NADPH oxidase cannot be ignored (Schimmel *et al*., 2002). However, experimental data demonstrated that treatment of NADPH oxidase inhibitor apocyanin was remained futile to give any protection to Resv treated cells (Figure 3A). Intriguingly, PEG-SOD treatment reduced both cell death (supplementary data 2B) and CM-H_2DCFDA (Fig. 3B) fluorescence after Resv treatment which confirmed mitochondrial superoxide production. Furthermore, pretreatment of cells with DMTU (.OH radical scavanger) gave significant protection to cells ($p< 0.001$) after Resv treatment thus proved the production of .OH and H_2O_2 (Fig.

3C). Therefore, the overall data signified that Resv treatment stimulated mitochondrial superoxide production which further through downstream reaction engendered H_2O_2 formation and .OH radical production.

Usually, generation of ROS oxidize GSH to GSSG and ultimately reduce the total GSH level. However, in vitro studies have also shown that a reduction in the intracellular GSH is necessary for the formation of ROS (Franco *et al*., 2007). Glutathione depletion has been shown to directly modulate both the loss of ($\Delta\Psi$m) and the activation of executioner caspases (Franco *et al*., 2007; Armstrong *et al.*, 2002). Hence, we sought to clarify the precise mechanism of GSH loss in Resv induced cell death. Time dependent study illustrated that Resv treatment depleted intracellular GSH content with initial hour and it continued with the time (Figure 4A). However, cell permeable potent ROS scavengers (PEG-SOD and PEG-Cat) failed to prevent the intracellular GSH depletion (Figure 4B), thus emphasized that intracellular GSH depletion was independent of ROS generation.

To gain a better insight into the control of GSH depletion in Resv treated cells, we analyzed whether two compounds, cystathionine and methionine, which are known to inhibit specific (synusoidal type) carriers responsible for reduced glutathione efflux from hepathocytes and U937 (Chow *et al*., 1995; Iu *et al*., 1996). As indicated in (Figure 4C), both the compounds minimized GSH depletion. Moreover, pretreatment of cells with extracellular thiols (NAC, GSH) and cystathionine prevented the loss of ($\Delta\Psi$m) (Figure 4D), ROS generation (Figure 4E) and simultaneously protected the cells after Resv treatment (Figure 4F). The data accentuated that, GSH efflux was one of the major events leading to the intracellular GSH depletion and apoptosis in Resv treated cells.

Next we investigated the missing link between GSH efflux and mitochondrial apoptotic signal. According to Honda *et al*, intracellular GSH depletion could stimulate Bax induced apoptosis in lung cancer (Honda *et al*., 2004). Here, we tried to find out in case of Resv treated cells whether GSH depletion could provoke mitochondrial Bax translocation resulting in activation of mitochondrial death cascade. Initially westernblot data demonstrated mitochondrial translocation of Bax protein (Figure 5A), which was further validated through confocal microscopic study. Confocal imaging signified mitochondrial Bax translocation as early with in 6 h of Resv treatment (Figure 5B). However, pretreatment of cystathionine or NAC profoundly prevented Bax translocation which was significantly reversed by BSO treatment (Figure 5B). Thus it delineated that mitochondrial Bax translocation which is a major apoptotic inducer was stimulated by GSH efflux in Resv treated cells. Additionally, Bax siRNA treatment revealed the importance of Bax in Resv induced apoptosis. Bax siRNA treatment inhibited cell death by 47 %, prevented the loss of ($\Delta\Psi$m), ROS generation and the downstream caspase activation (Figure 6); therefore, it confirmed that mitochondrial Bax translocation in Resv treated U937 cell stimulated the loss of ($\Delta\Psi$m) followed by ROS generation and caspase activation which finally triggered apoptosis. However, as BSO itself failed to instigate apoptosis despite mitochondrial Bax translocation and ROS accumulation so it could be concluded that mitochondrial Bax translocation and ROS generations are the important linker molecule in Resv induced apoptotic signal transduction cascade but not sufficient to induce resveratrol-provoked caspase activation and apoptosis alone.

Now from these above sets of data a potential signal transduction cascade can be sketched in Resv induced apoptosis where GSH depletion was playing the central role.

In the niche of GSH efflux, mitochondrial Bax translocation amplified the whole apoptotic signal; initiated from dissipation of ($\Delta\Psi$m), ROS production ultimately leading to the downstream caspase activation and cell death. Thus Resv treatment provoked GSH extrusion and mitochondrial Bax translocation to accomplish apoptosis in U937 cell line.

Acknowledgements

We thank the reviewers for valuable suggestions for the improvement of the manuscript. The authors are grateful to Prof. P.K. Mitra, Director, IPGME&R, Kolkata for providing infrastructural facilities as well as constant encouragement.

References

Armstrong JS and Jones DP (2002) Glutathione depletion enforces the mitochondrial permeability transition and causes cell death in HL60 cells that overexpress Bcl-2. *Faseb J* **16**: 1263–1265.

Bradford MM (1976) A rapid and sensitive method for the quantitation of microgram quantities utilizing the principle of protein dye binding. *Anal Biochem*; **72**:248-54.

Chow SC, Peters I and Orrenius S (1995) Reevaluation of the role of de novo protein synthesis in rat thymocytes apoptosis. *Exp Cell Res* **216**: 149–159.

Franco R and Cidlowski JA (2006) SLCO/OATP-like transport of glutathione in FasL-induced apoptosis. *J Biol Chem* **281**: 29542–29557.

Franco R, Panayiotidis MI and Cidlowski JA (2007) Glutathione Depletion Is Necessary for Apoptosis in Lymphoid Cells Independent of Reactive Oxygen Species Formation. *J Biol Chem* **282**: 30452–30465.

Ghibelli L, Fanelli C, Rotilio G, Lafavia E, Coppola S, Colussi C, Civitareale P and Ciriolo MR (1998) Rescue of cells from apoptosis by inhibition of active GSH extrusion *FASEB J* **12**: 479–486.

Guha P, Dey A, Dhyani MV, Sen R, Chatterjee M, Chattopadhyay S and Bandyopadhyay SK. Calpain and Caspase Orchestrated Death Signal to Accomplish Apoptosis Induced by Resveratrol and its Novel Analog HST-1 in Cancer Cells *J Pharmacol Exp Ther* **334:** 381-394.

Hammond CL, Madejczyk MS and Ballatori N (2004) Activation of plasma membrane reduced glutathione transport in death receptor apoptosis of HepG2 cells. *Toxicol Appl Pharmacol* **195**: 12–22.

He YY, Huang JL, Ramirez DC and Chignell CF (2003) Role of reduced glutathione efflux in apoptosis of immortalized human keratinocytes induced by UVA. *J Biol Chem* **278**: 8058–8064.

Honda T, Coppola S, Ghibelli L, Cho SH, Kagawa S, Spurgers KB, Brisbay SM, Roth JA, Meyn RE, Fang B and McDonnell TJ (2004) GSH depletion enhances adenoviral bax-induced apoptosis in lung cancer cells. *Cancer Gene Therapy* **11**: 249–255.

Iu SC, Sun WM, Yi J, Ookthens M, Sze G and Kaplowitz N (1996) Role of two recently cloned rat liver GSH transporters in the ubiquitous transport of GSH mammalian cells. *J Clin Invest* **97**: 1488–1496.

Kirkland RA and Franklin JL (2007) Bax affects production of reactive oxygen by the mitochondria of non-apoptotic neurons *Exp Neurol*. **204**: 458-461.

Macho A, Hirsch T, Marzo I, Marchetti P, Dallaporta B, Susin SA, Zamzami N and Kroemer C (1997) Glutathione Depletion Is an Early and Calcium Elevation Is a Late Event of Thymocyte Apoptosis. *J Immunol* **158**: 4612-4619.

Meister A and Anderson ME (1983) Glutathione. *Annu Rev Biochem* **52**: 711-760.

Mohan J, Gandhi AA, Bhavya BC, Rashmi R, Karunagaran D, Indu R and Kumar TRS (2006) Caspase-2 Triggers Bax-Bak- dependent and –independent Cell Death in Colon Cancer Cells Treated with Resveratrol. *J Biol Chem* **281**: 17599–17611.

Reed DJ (1990) Glutathione: Toxicological implications. *Annu Rev Pharmacol Toxicol* **30**: 603- 631.

Schimmel M and Bauer G (2002) Proapoptotic and redox state-related signaling of reactive oxygen species generated by transformed fibroblasts. *Oncogene* **21**: 5886 – 5896.

van den Dobbelsteen DJ, Nobel CS, Schlegel J, Cotgreave IA, Orrenius S and Slater AF (1996) Rapid and specific efflux of reduced glutathione during apoptosis induced by Anti-Fas/APO-1 antibody. *J Biol Chem* **271**: 15420–15427.

Footnotes

Source of Financial Support: The work was financially supported by Life Science Research Board, Defence Research & Development Organisation (DRDO), Govt. of India and Department of Science and Technology (DST), Govt. of India.

P. G. and **A. D.** are recipients of fellowship from the DST and LSRB, DRDO, Govt. of India

Person to Receive Reprint Request: Dr. Sandip K. Bandyopadhyay, Department of Biochemistry, Dr. B.C. Roy Post Graduate Institute of Basic medical Sciences & IPGME&R, 244B, Acharya Jagadish Chandra Bose Road, Kolkata-700 020, India.

Phone: 91-033-22234838; E-Mail: sandipkpc@gmail.com.

Legends for Figures

Figure 1. Resv treatment induced apoptosis in U937 cell line.

(A) Cell viability study was carried out on U937 cell lines using the CellTiter-Glo® Luminescent Cell Viability Assay kit. The data represented a time dependent (12, 24, 48, 72 h) effect of Resv at its varying doses. FACS data elucidated apoptosis by Anexin V/ PI assay (B), TUNEL assay (C) and caspase 3 activation assay (D). The flowcytometric data are representative of three different experiments.

Figure 2. Resv treatment induced ROS generation and modulated dissipation of mitochondrial membrane potential.

The U937 cells were treated with Resv (50μM) and dissipation of mitochondrial membrane potential (A) and ROS generation (B) were studied spectroflurimetrically in a time dependent manner. The data are the representative of 6 experiments.

Figure 3. Resv treatment triggered oxidative burst in mitochondria and production of ROS resulted in the deleterious effects.

U937 cells were treated with Resv (50μM) and the role different ROS was evaluated by using different inhibitors and fluorescent dyes. Apocyanin (200μM) treatment (A) denoted the role of NADPH oxidase. Staining of cells with CM-H2DCFDA explored the generation of H_2O_2 which was validated by pretreatment of cells with potent cell permeable antioxidants PEG-SOD (800 Unit/ ml), PEG-Cat (3000 Unit/ ml) and NAC (8mM) (B). DMTU (6 mM) (C) pretreatment enumerated the probable role of hydroxyl

radical in Resv treated cell death. The role of singlet oxygen was evaluated by using singlet oxygen sensor green dye (D). L-NAME (1mM) (E) pretreatment enumerated the probable role of nitric oxide in Resv treated cell death. The data are represented as mean ± SD (n= 6). ***P < 0.001 versus Resv treated group.

Figure 4. GSH efflux and subsequent conversion of GSH to GSSG positively controlled ROS generation.

After Resv treatment a time dependent study on intracellular GSH depletion was evaluated (A). The role of cell permeable antioxidants in GSH depletion was explored (B).The impact of cystathionine (1mM) and methionine (1mM) on GSH efflux was evaluated in Resv treated U937 cells (C). The role of GSH efflux on the loss of mitochondrial membrane potential (D), ROS generation (E) and cell death (F) was evaluated. The data are represented as mean ± SD (n= 6). ***P < 0.001 versus Resv treated group.

Figure 5. Resv induced Bax translocation to mitochondria was modulated by GSH depletion.

Effects of Bax siRNA on mitochondrial Bax translocation was evaluated after 24 h of treatment by western blot analysis (A). COX IV was the representative of mitochondrial loading control and β-actin as cytosolic loading control in the western blot data. The U937 cells were treated with Resv and different inhibitors then translocation of cytosolic Bax to mitochondria was evaluated through confocal imaging after 6 h of Resv (50μM) treatment. The mitochondria was stained by COX IV alexa fluor 488 monoclonal

antibody (green) and Bax was stained with Alexa fluor 594 anti mouse secondary antibody (red). The colocalization of Bax protein to mitochondria was evaluated by merged picture. The bar represents the magnification which was 20μm.

Figure 6. Bax translocation triggered mitochondrial death signal.

Effects of Bax siRNA on mitochondrial Bax translocation was evaluated after 24 h of treatment by TaqMan realtime PCR (A). (B) Represented the effect of Bax siRNA on cell death 48 h after Resv treatment. Treatment of Bax siRNA prevented caspase 3 activation (C), ROS generation (D) and loss of mitochondrial memebrane potential (E). The data are represented as mean ± SD (n= 6). ***P < 0.001 versus Resv treated group.

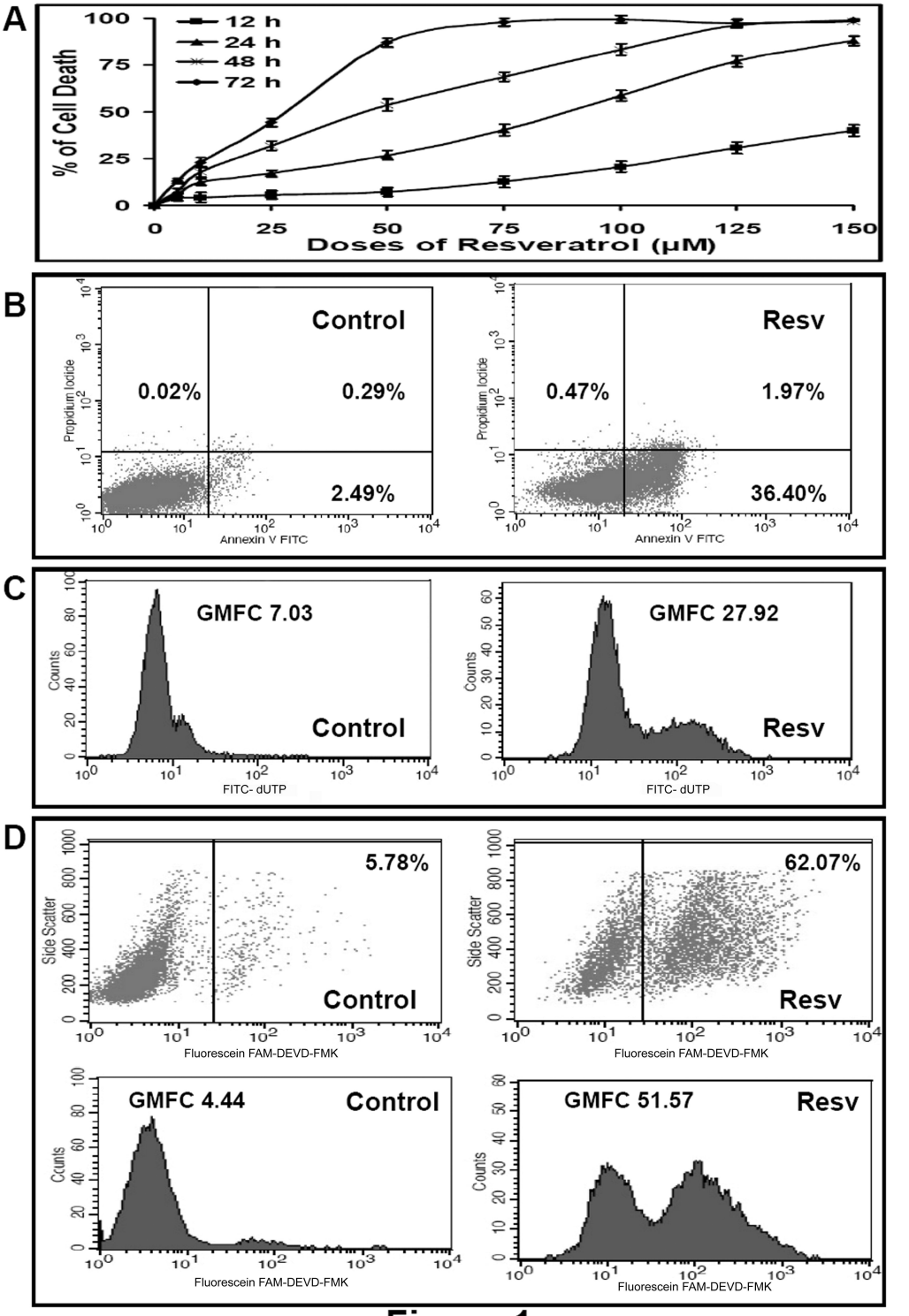
A
12 h
24 h
48 h
72 h
% of Cell Death
Doses of Resveratrol (μM)
B
Control
0.02%
0.29%
2.49%
Resv
0.47%
1.97%
36.40%
Propidium Iodide
Annexin V FITC
C
GMFC 7.03
Control
GMFC 27.92
Resv
Counts
FITC- dUTP
D
5.78%
Control
62.07%
Resv
Side Scatter
Fluorescein FAM-DEVD-FMK
GMFC 4.44
Control
GMFC 51.57
Resv
Counts

Figure 1

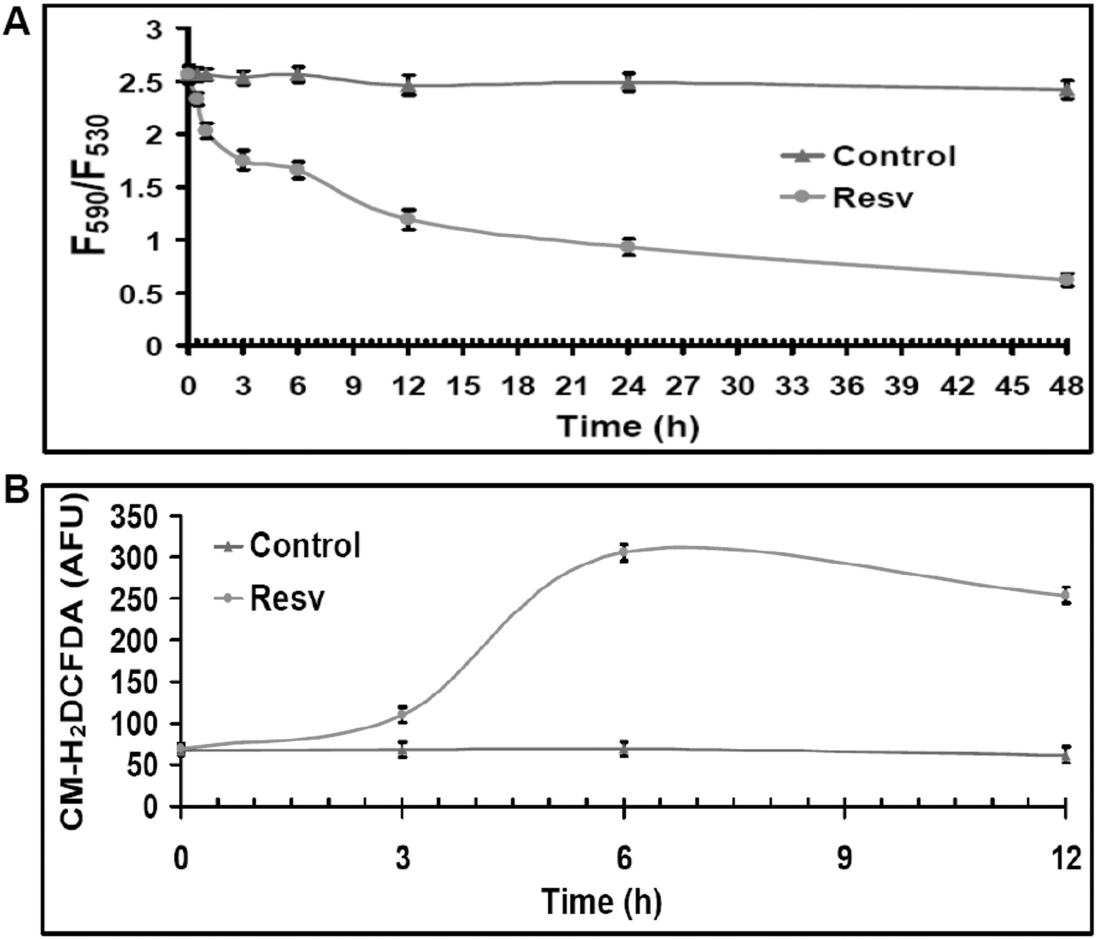
A
3
2.5
2
1.5
1
0.5
0
F_{590}/F_{530}
Control
Resv
0 3 6 9 12 15 18 21 24 27 30 33 36 39 42 45 48
Time (h)
B
350
300
250
200
150
100
50
0
CM-H_2DCFDA (AFU)
Control
Resv
0 3 6 9 12
Time (h)

Figure 2

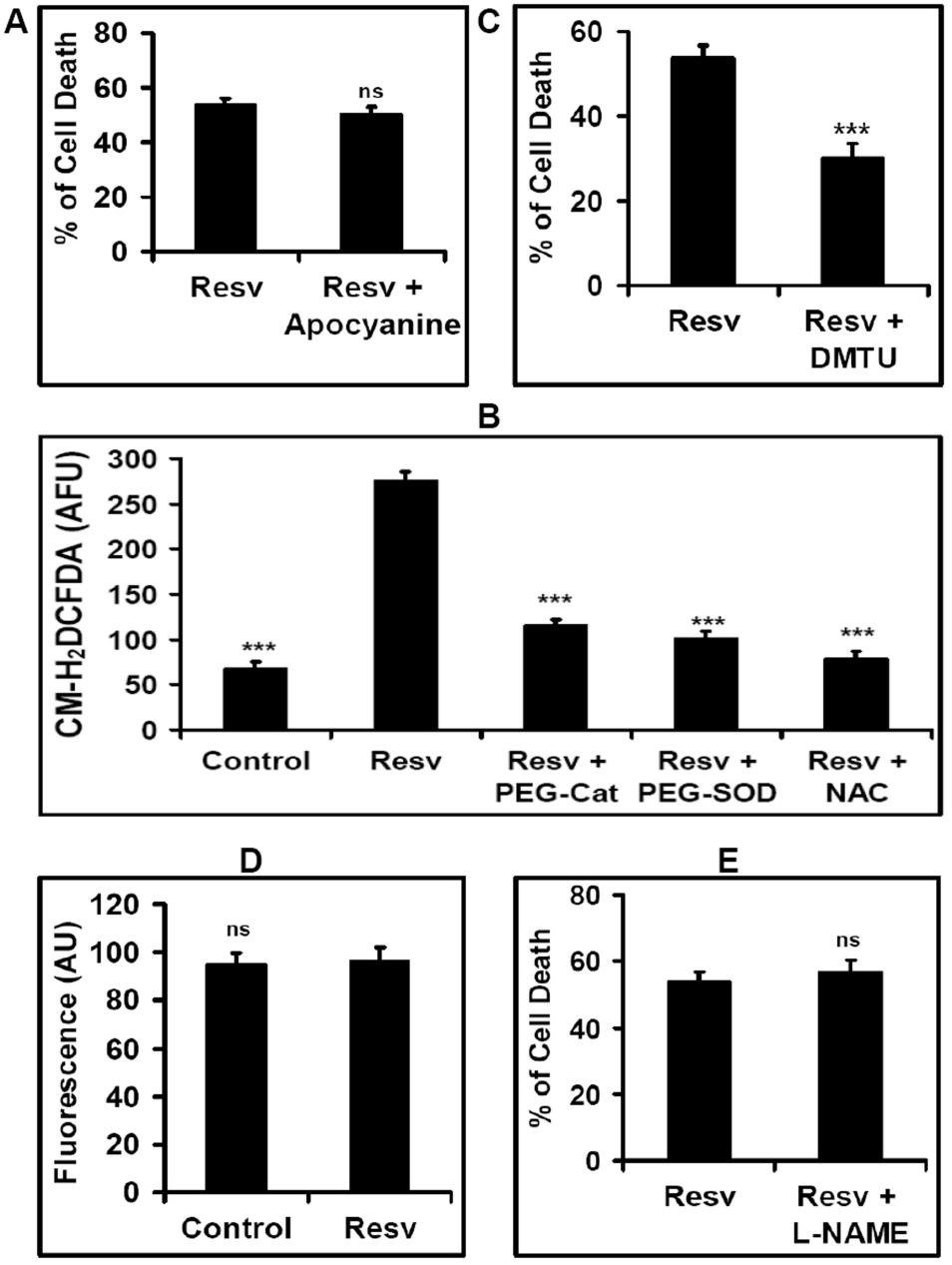
A
% of Cell Death
80
60
40
20
0
ns
Resv
Resv + Apocyanine
C
% of Cell Death
60
40
20
0
***
Resv
Resv + DMTU
B
CM-H2DCFDA (AFU)
300
250
200
150
100
50
0
***
***
***
***
Control
Resv
Resv + PEG-Cat
Resv + PEG-SOD
Resv + NAC
D
Fluorescence (AU)
120
100
80
60
40
20
0
ns
Control
Resv
E
% of Cell Death
80
60
40
20
0
ns
Resv
Resv + L-NAME

Figure 3

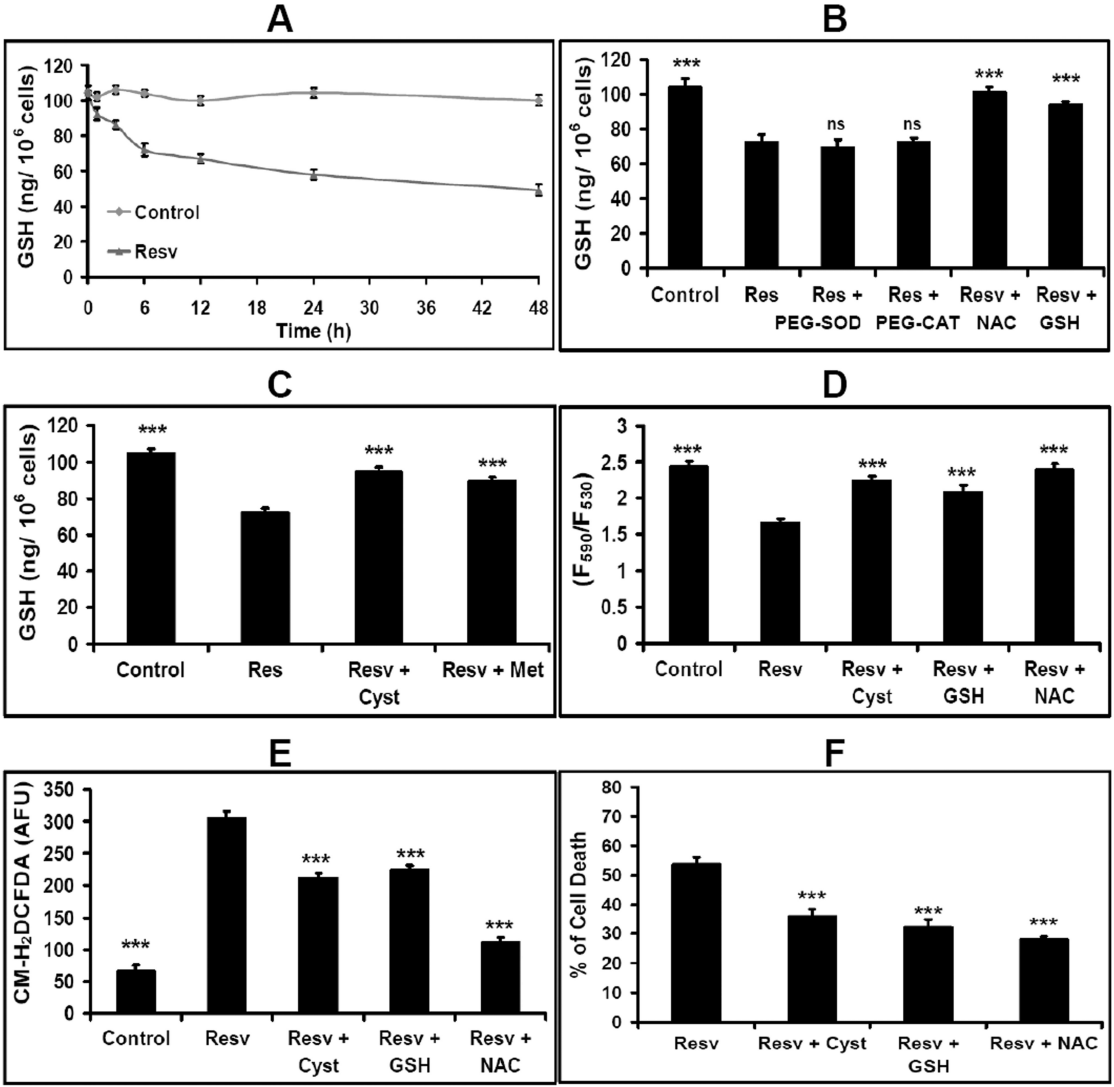
A
GSH (ng/ 10^6 cells)
120
100
80
60
40
20
0
Control
Resv
0
6
12
18
24
30
36
42
48
Time (h)
B
GSH (ng/ 10^6 cells)
***
ns
ns
***
***
Control
Res
Res + PEG-SOD
Res + PEG-CAT
Resv + NAC
Resv + GSH
C
GSH (ng/ 10^6 cells)
***
***
***
Control
Res
Resv + Cyst
Resv + Met
D
(F590/F530)
3
2.5
2
1.5
1
0.5
0
***
***
***
***
Control
Resv
Resv + Cyst
Resv + GSH
Resv + NAC
E
CM-H2DCFDA (AFU)
350
300
250
200
150
100
50
0
***
***
***
Control
Resv
Resv + Cyst
Resv + GSH
Resv + NAC
F
% of Cell Death
80
70
60
50
40
30
20
10
0
***
***
***
Resv
Resv + Cyst
Resv + GSH
Resv + NAC

Figure 4

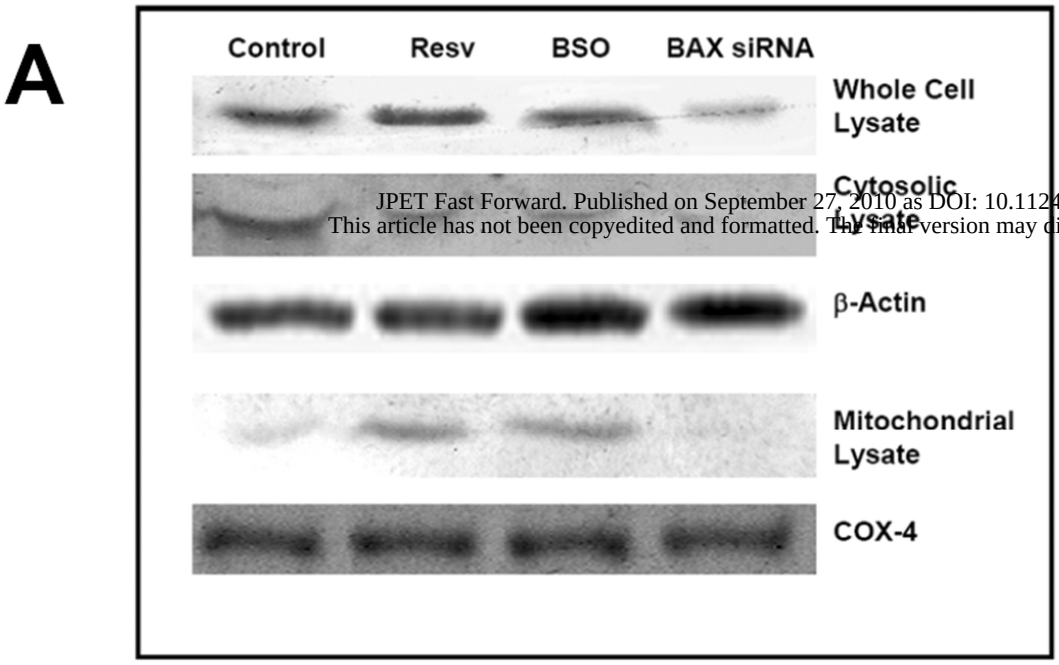

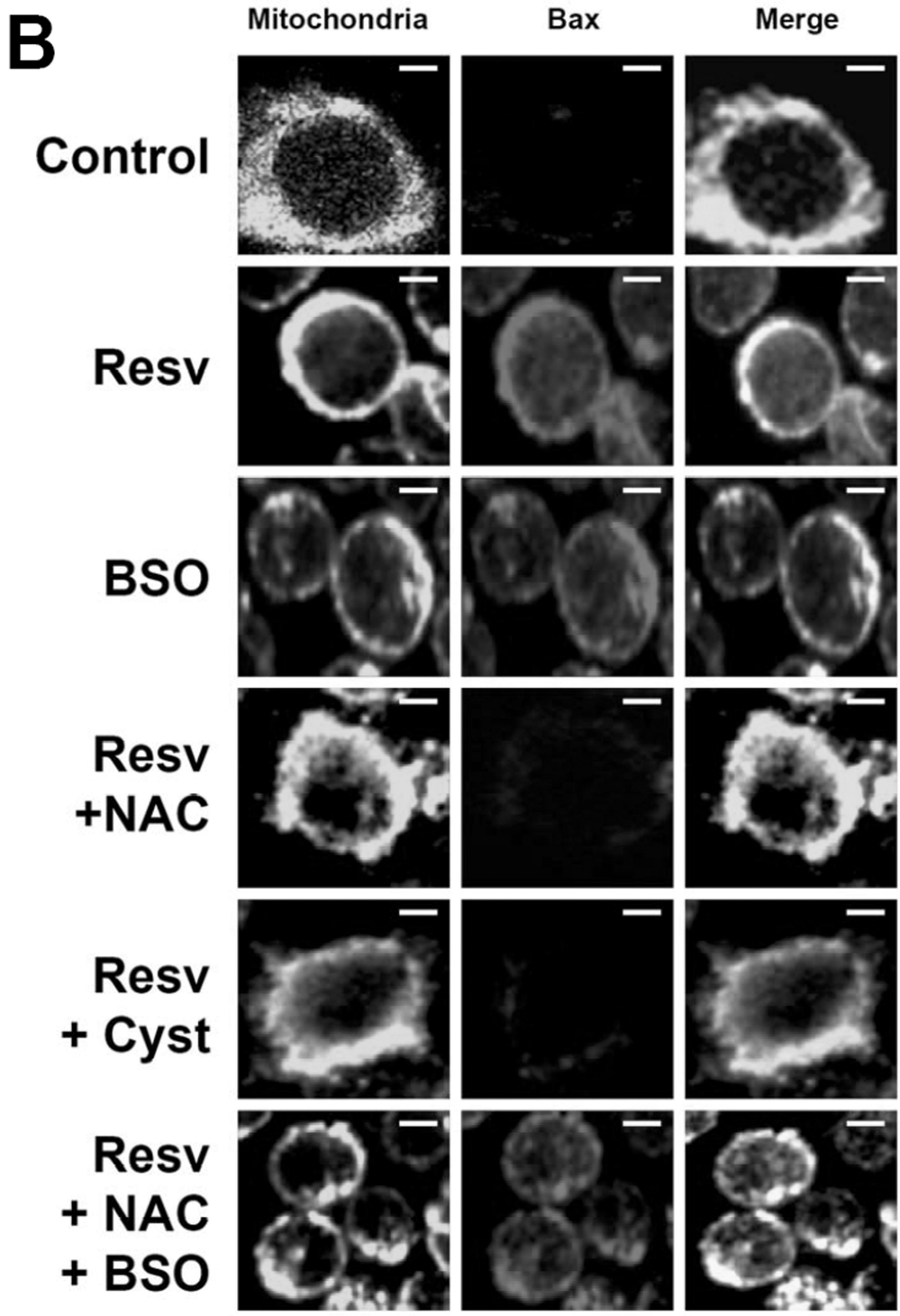

Figure 5

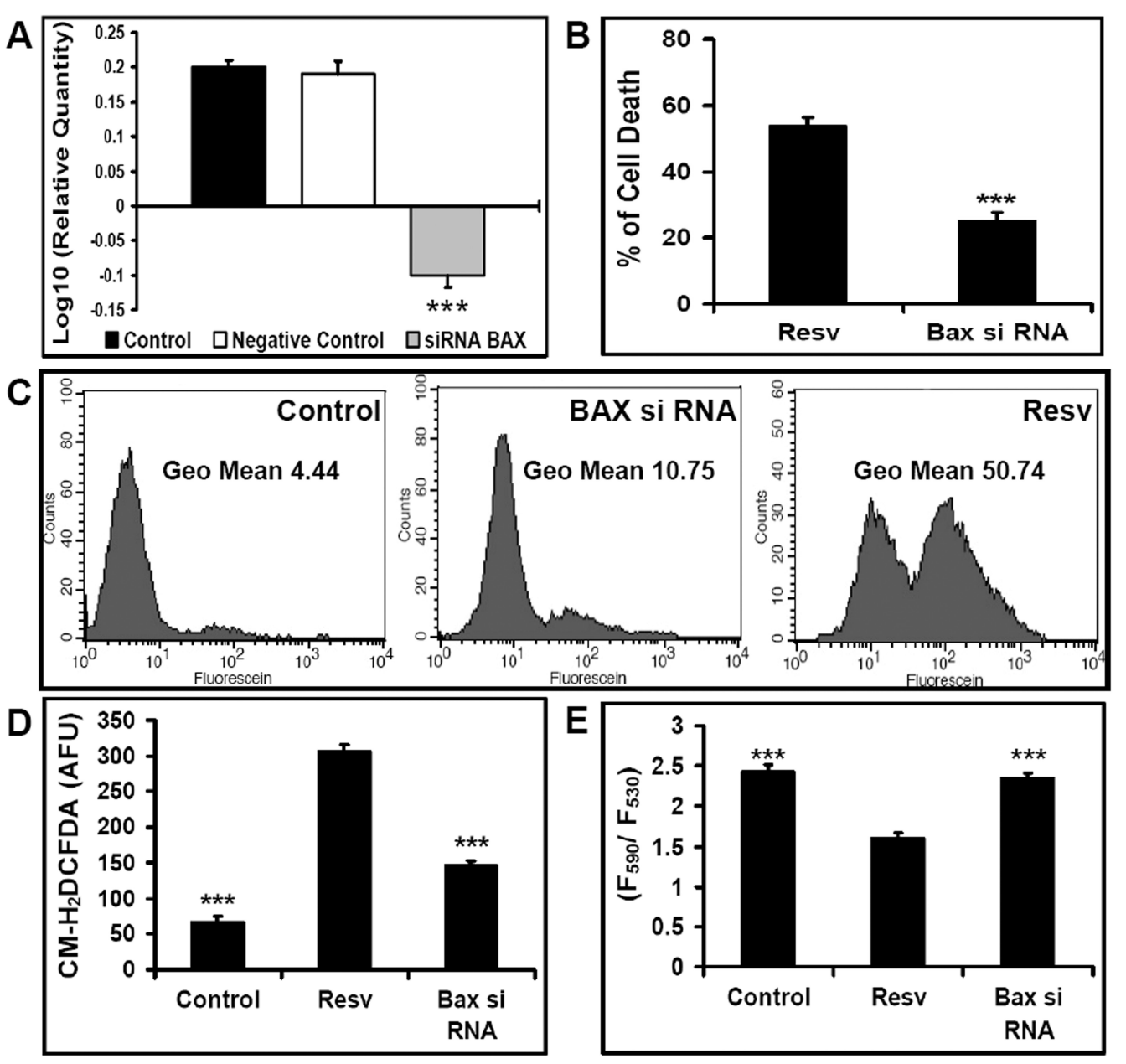
A
Log10 (Relative Quantity)
0.25
0.2
0.15
0.1
0.05
0
-0.05
-0.1
-0.15
***
Control
Negative Control
siRNA BAX
B
% of Cell Death
80
60
40
20
0
***
Resv
Bax si RNA
C
Control
Geo Mean 4.44
BAX si RNA
Geo Mean 10.75
Resv
Geo Mean 50.74
Counts
Fluorescein
D
CM-H2DCFDA (AFU)
350
300
250
200
150
100
50
0
***
***
Control
Resv
Bax si RNA
E
(F590/ F530)
3
2.5
2
1.5
1
0.5
0
***
***
Control
Resv
Bax si RNA

Figure 6